# Discrete and Continuous Spectra of the Barotropic Quasigeostrophic Vorticity Model. Part I

MINGHUA ZHANG

*Institute for Terrestrial and Planetary Atmospheres, State University of New York at Stony Brook, Stony Brook, New York*

QINGCUN ZENG

*Institute of Atmospheric Physics, Academia Sinica, Beijing, China*

(Manuscript received 9 October 1995, in final form 4 February 1997)

ABSTRACT

The evolution processes of small disturbances in an arbitrary basic flow can be expressed as a combination of spectral functions of the discrete spectra and continuous spectrum of a model that bear distinctly different evolutionary characteristics. Using the linearized barotropic quasigeostrophic vorticity model, this study formulates the discrete spectral solution into a form that is consistent with traditional normal modes in time and space, and the continuous spectral solution into a form with the continuum covering the range between minimum and maximum zonal angular velocities. An estimation of the bounds of the spectral points is derived to complement those derived from integral constraints. A theorem is given to describe the possible number of discrete spectral points away from the continuum.

The theoretical analysis is then used to aid the numerical identification and interpretation of discrete and continuous spectra of the model with realistic atmospheric basic zonal flows. It is shown that neutral spectral points correspond to either ultralong waves with global meridional coverage or synoptic-scale waves in low latitudes. The unstable spectral points correspond to localized waves with developing or decaying timescales longer than 2 weeks. Structures of spectral function of the continuum are also presented and discussed. They are shown to restrict on one side to the critical latitude and on the other side to the jet core under certain conditions.

## 1. Introduction

Since Rossby's pioneer work of longwave dynamics, the normal mode method has been widely used in the study of evolutionary processes of small atmospheric disturbances (e.g., Charney 1947). Many studies have dealt with the frequencies, structures, and the unstable increasing growth rates of these normal modes (characteristic waves). The results are then applied to explain the propagation, development, or decay of atmospheric disturbances. Normal modes, however, in general do not constitute a complete set of basis functions for atmospheric disturbances (Case 1960; Pedlosky 1964a; Burger 1966; Zeng 1979; Farrell 1982, 1984; Held 1985; Zeng et al. 1986; Lu et al. 1986). They can only describe propagating waves and exponentially growing or decaying unstable waves, not nonmodal solutions. The nonmodal solution has been shown to exclusively describe the behavior of linear disturbances in some very simple models (Yamagata 1976; Tung 1983) and dominate the behavior of disturbances in others (Farrell 1982). The most distinctive feature of a nonmodal solution is its transient and dispersive behavior with the disturbance continuously sheared by the basic flow. Differential advection of disturbances by the basic flow, as described by a nonmodal solution, is able to either cause rapid development or rapid decay of atmospheric disturbances (Farrell 1985).

Simultaneous formulation of both discrete and continuous spectrum solutions has been discussed to various degrees in several studies (e.g., Yanai and Nitta 1968; Held 1985; Held et al. 1985; Farrell 1989). A typical approach is to solve an initial value problem using Laplace transformation. The inverse of the Laplace integration gives rise to discrete modes around the removable singularities (modal solution) and continuous spectrum along cut lines of the transformed streamfunction (nonmodal solution). The theory, however, has not been complete in terms of how discrete modes in this procedure actually conform with the traditional normal modes in their spatial structures and what the range of the continuous spectrum should be.

The purpose of this paper is to advance the theory of

*Corresponding author address:* Dr. Minghua Zhang, Institute for Terrestrial and Planetary Atmospheres, State University of New York at Stony Brook, Stony Brook, NY 11794-5000.
E-mail: mzhang@atmsci.msrc.sunysb.edu

the discrete and continuous spectra of a model and to interpret the observed atmospheric disturbances. In the following two sections, we first formulate a compact form of the solution of the initial value problem of the barotropic quasigeostrophic vorticity model on the sphere. The theoretical analysis is then used to numerically identify the two sets of spectra in section 4, which is a necessary step toward quantitatively using the concept of spectra for practical applications, such as initialization for numerical weather forecasts. The calculated results of the discrete and continuous spectra of the atmospheric model are presented and discussed in sections 5 and 6. They provide a basis to understand which disturbance structures can propagate and grow exponentially in the atmosphere and which cannot. Actual projection of the observed disturbances onto these spectral functions, and interpretation of their evolution following the theory, will be described in a companion paper. The last section contains a summary of this paper.

## 2. Initial-value problem, spectra, and spectral functions

The barotropic quasigeostrophic vorticity model linearized with respect to a zonal basic flow $\bar{v}_\lambda$ on a sphere is written as

$$\left(\frac{\partial}{\partial t} + \frac{\bar{v}_\lambda}{a\sin\theta}\frac{\partial}{\partial\lambda}\right)\zeta' + v'_\theta\frac{\partial\bar{\zeta}}{a\partial\theta} = 0, \tag{1}$$

where

$$\zeta' = \frac{1}{a^2\sin\theta}\frac{\partial}{\partial\theta}\sin\theta\frac{\partial\psi'}{\partial\theta} + \frac{1}{a^2\sin^2\theta}\frac{\partial^2\psi'}{\partial\lambda^2}, \tag{2}$$

$$v'_\theta = -\frac{\partial\psi'}{a\sin\theta\partial\lambda}, \tag{3}$$

and

$$\bar{\zeta} = \frac{1}{a\sin\theta}\frac{\partial\sin\theta\bar{v}_\lambda}{\partial\theta} + 2\omega\cos\theta. \tag{4}$$

Here, $\lambda$ and $\theta$ are longitude and colatitude, respectively. The initial and boundary conditions are $\zeta'|_{t=0} = \zeta'_0 = \sum \zeta_0^k e^{ik\lambda}$ and $\psi' = 0$ at $\theta = \theta_1$ and $\theta = \theta_2$. Looking at a single zonal wavenumber component $\psi^k$,

$$\psi'(\lambda, \theta, t) = \sum_{k=-\infty}^{+\infty}\psi^k(\theta, t)e^{ik\lambda}, \tag{5}$$

with Laplace transformation

$$\tilde{\psi}^k(\theta, c) = \int_0^\infty \psi^k(\theta, t)e^{ikct}\,dt, \tag{6}$$

for sufficiently large $c_i$, $\tilde{\psi}^k(\theta, c)$ becomes an analytic function of $c$. Here $\tilde{\psi}^k(\theta, c)$ satisfies the equation

$$\left(\bar{\lambda}(\theta) - c\right)\left(\frac{1}{\sin\theta}\frac{d}{d\theta}\sin\theta\frac{d\tilde{\psi}^k}{d\theta} - \frac{k^2}{\sin^2\theta}\tilde{\psi}^k\right) - \frac{1}{\sin\theta}\frac{d\bar{\zeta}}{d\theta}\tilde{\psi}^k = \frac{1}{ik}\zeta_0^k(\theta) \tag{7}$$

with

$$\tilde{\psi}^k|_{\theta=\theta_1} = \tilde{\psi}^k|_{\theta=\theta_2} = 0, \tag{8}$$

where $\bar{\lambda}(\theta) = \bar{v}_\lambda/(a\sin\theta)$. The inverse Laplace transformation gives the solution for $\psi^k(\theta, t)$:

$$\psi^k(\theta, t) = \frac{k}{2\pi}\int_\Gamma \tilde{\psi}^k(\theta, c)e^{-ikct}\,dc = \int_{-\infty+s_0 i}^{+\infty+s_0 i}\tilde{\psi}^k(\theta, c)e^{-ikct}\,dc, \tag{9}$$

in which $s_0$ is sufficiently large and $\theta \in [\theta_1, \theta_2]$.

Previous studies (e.g., Case 1960; Pedlosky 1964a; Burger 1966) have pointed out that the above integration of $\tilde{\psi}^k(\theta, c)$ along $\Gamma$ (Fig. 1a) can be replaced by the sum of integration along the isolated poles of $\tilde{\psi}^k(\theta, c)$ on the $c$ plane, which yields a time dependence $\exp(-ikc_r^k t)$ in the solution, and integration along a continuous line, which represents the continuous spectrum of the solution. In the following, we first discuss the spatial structures of the integration along the isolated poles of $\tilde{\psi}^k(\theta, c)$ and then discuss the range of the continuous spectrum. For the Eady model, Pedlosky (1964a) showed that spatial distribution of the integration around the poles is the same as the two Eady modes.

Given two independent solutions of the homogeneous form of (7) and (8) as $\psi_1(\theta, c)$ and $\psi_2(\theta, c)$, $\tilde{\psi}^k(\theta, c)$ can be expressed as

$$\tilde{\psi}^k(\theta, c) = \int_{\theta_1}^{\theta_2} G^k(\theta, \theta', c)\frac{\zeta_0(\theta')}{ik\left[\bar{\lambda}(\theta') - c\right]}\,d\theta', \tag{10}$$

where $G^k(\theta, \theta', c)$ is the Green's function related with $\psi_1(\theta, c)$ and $\psi_2(\theta, c)$ as in the appendix. Looking at the analytical continuation of $\tilde{\psi}^k(\theta, c)$ to the whole $c$ plane, it can be shown from (7)–(8) that

$$\lim_{|c|\to\infty}\tilde{\psi}^k(\theta, c) \to 0. \tag{11}$$

The Jordan lemma extension assures that integration (9) along the infinite contour $\Gamma$ (from $-\infty + s_0 i$ to $\infty + s_0 i$) equals to a limit integration along $C_\Gamma + C_R$ with $R \to \infty$ (see Fig. 1a), that is,

$$\psi^k(\theta, t) = \lim_{R\to\infty}\frac{k}{2\pi}\oint_{C_\Gamma + C_R}\tilde{\psi}^k(\theta, c)e^{-ikct}\,dc, \tag{12}$$

where $C_R$ is a partial circle with radius $R$, and $C_\Gamma$ is the part of $\Gamma$ intercepted by $C_R$ (Fig. 1a).

The Green's function $G^k(\theta, \theta', c)$ only has removable singularities when $c$ is beyond $[\bar{\lambda}_{\min}, \bar{\lambda}_{\max}]$ (see appen-

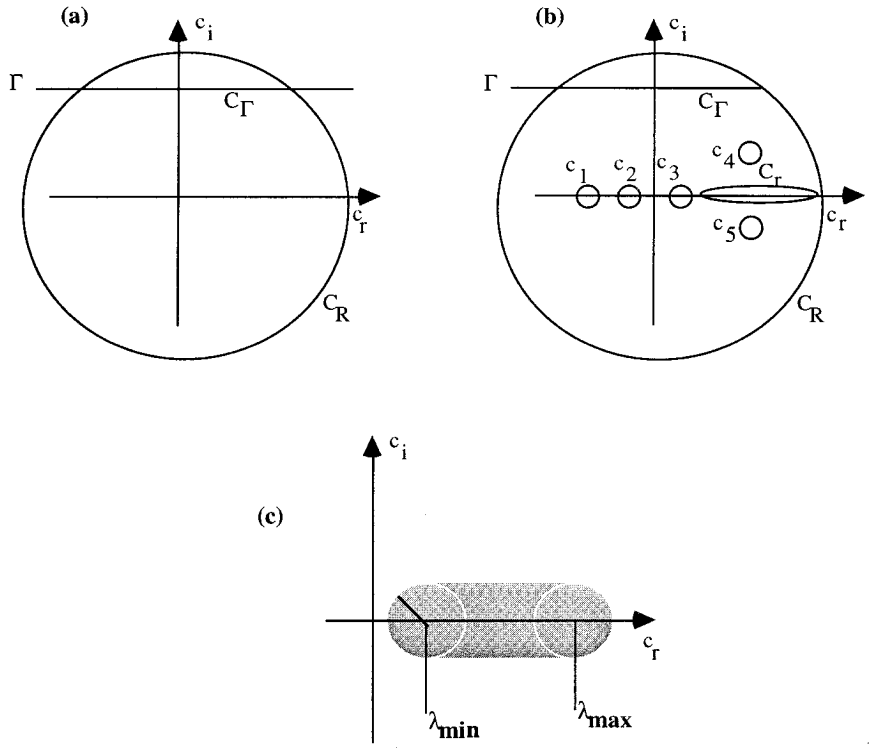


FIG. 1. (a) and (b) Schematic picture of integral contours. (c) Existing domain of the discrete spectral points.

dix); integration of $\tilde{\psi}^k(\theta, c)$ around these singularities yields

$$\sum_l \oint_{C_l} \left[ \int_{\theta_1}^{\theta_2} \frac{G^k(\theta, \theta', c)}{2\pi i \left[ \bar{\lambda}(\theta') - c \right]} \zeta_0^k(\theta')\, d\theta' \right] e^{-ikct}\, dc,$$

$$= \int_{\theta_1}^{\theta_2} \left\{ \sum_l \oint_{C_l} \frac{G^k(\theta, \theta', c)}{2\pi i \left[ \bar{\lambda}(\theta') - c \right]} e^{-ikct}\, dc \right\} \zeta_0^k(\theta')\, d\theta'. \tag{13}$$

Write (residue theorem)

$$\sum_l \oint_{C_l} \frac{G^k(\theta, \theta', c)}{2\pi i \left[ \bar{\lambda}(\theta') - c \right]} e^{-ikct}\, dc = \sum_l \tilde{G}_l^k(\theta, \theta', c_l^k) e^{-ikc_l^k t}, \tag{14}$$

where $\tilde{G}_l^k$ is expressed as

$$\tilde{G}_l^k(\theta, \theta', c) = \begin{cases} F(c_l^k)\tilde{G}_{l,1}^k(\theta', c) G_{l,2}^k(\theta, c), & \text{if } \theta \geq \theta' \\ F(c_l^k)\tilde{G}_{l,2}^k(\theta', c) G_{l,1}^k(\theta, c), & \text{if } \theta < \theta', \end{cases} \tag{15}$$

integrations in (13) become

$$\psi_d^k(\theta, t) = \sum_l \left\{ \left[ \int_{\theta_1}^{\theta} F(c_l^k)\tilde{G}_{l,1}^k(\theta', c_l^k)\zeta_0^k(\theta')\, d\theta' \right] G_{l,2}^k(\theta, c_l^k) + \left[ \int_{\theta}^{\theta_2} F(c_l^k)\tilde{G}_{l,2}^k(\theta', c_l^k)\zeta_0^k(\theta')\, d\theta' \right] G_{l,1}^k(\theta, c_l^k) \right\} \times e^{-ikc_l^k t}. \tag{16}$$

Define

$$A_l^k G_l^k(\theta, c_l^k) = \left[ \int_{\theta_1}^{\theta} F(c_l^k)\tilde{G}_{l,1}^k(\theta', c_l^k)\zeta_0^k(\theta')\, d\theta' \right] G_{l,2}^k(\theta, c_l^k) + \left[ \int_{\theta}^{\theta_2} F(c_l^k)\tilde{G}_{l,2}^k(\theta', c_l^k)\zeta_0^k(\theta')\, d\theta' \right] G_{l,1}^k(\theta, c_l^k). \tag{17}$$

It can be shown that $G_l^k(\theta, c_l^k)$ satisfies the homogeneous form of Eq. (7), it also satisfies the homogeneous boundary conditions at $\theta = \theta_1$ and $\theta = \theta_2$. Therefore $G_l^k(\theta, c_l^k)$ is actually an eigenfunction of the following eigenvalue problem:

$$\left(\bar{\lambda}(\theta) - c_l^k\right)\left(\frac{1}{\sin\theta}\frac{d}{d\theta}\sin\theta\frac{dG_l^k}{d\theta} - \frac{k^2}{\sin^2\theta}G_l^k\right) - \frac{1}{\sin\theta}\frac{d\bar{\zeta}}{d\theta}G_l^k = 0, \quad (18)$$

$$G_l^k\big|_{\theta_1;\theta_2} = 0. \quad (19)$$

The zero points of $D(c)$ in the appendix are the singularities of $G(\theta, \theta', c)$ and hence are the eigenvalues $c_l^k$. Since these zero points are isolated on the complex $c$ plane beyond $[\bar{\lambda}_{\min}, \bar{\lambda}_{\max}]$, they are defined as discrete spectra of the model. The eigenfunctions $G_l^k(\theta, c_l^k)$ are defined as the discrete spectral functions of the model. Here, $\psi_d^k$ is called the discrete spectrum disturbance

$$\psi_d^k = \sum_l A_l^k G_l^k(\theta) e^{-ikc_l^k t}.$$

According to the Cauchy theorem, the inverse Laplace integration equals to the sum of those around the isolated poles of $\tilde{\psi}^k(\theta, c)$ plus integration along the cut lines of $\tilde{\psi}^k(\theta, c)$, if it has branch points on the $c$ plane. When $c$ belongs to $[\bar{\lambda}_{\min}, \bar{\lambda}_{\max}]$, the two homogeneous solutions of $\psi_1(\theta, c)$ and $\psi_2(\theta, c)$ indeed contain branch points at $\bar{\lambda}(\theta) = c$. If $d\bar{\lambda}/d\theta \neq 0$ at $\theta$, then a series expansion of the solution around $\theta$ would yield an analytic solution of $\psi_1(\theta, c)$ and a second solution from the Frobineis method,

$$\psi_2(\theta, c) = g\psi_1(\theta, c)\ln\left[\bar{\lambda}(\theta) - c\right] + \phi_1(\theta, c), \quad (20)$$

where $g$ is a constant and $\phi$ is an analytic function of $c$. Therefore, $c = \bar{\lambda}(\theta)$ is a logarithmic branch point of $\psi_2(\theta, c)$. Furthermore, if the two homogeneous solutions can be analytically extended to the boundaries, then in the Green's function $G(\theta, \theta', c)$ (see appendix), $c = \bar{\lambda}(\theta_1)$ and $c = \bar{\lambda}(\theta_2)$ are also branch points. However, $G_1(\theta, c)$ in the numerator of $G(\theta, \theta', c)$ in (A1) can been arranged to only contain $\ln\{[c - \bar{\lambda}(\theta)]/[c - \bar{\lambda}(\theta_1)]\}$. Therefore, a cut line connecting $c = \bar{\lambda}(\theta)$ and $c = \bar{\lambda}(\theta_1)$ is sufficient to form a single-value $G_1(\theta, c)$ on the $c$ plane. Similarly, a cut line connecting $c = \bar{\lambda}(\theta)$ and $c = \bar{\lambda}(\theta_2)$ can be taken for $G_2(\theta, c)$, and a cut line connecting $c = \bar{\lambda}(\theta_1)$ and $c = \bar{\lambda}(\theta_2)$ for $D(c)$. If the solutions at the boundaries cannot be written as analytical continuation of the expansion series at $\bar{\lambda}(\theta) = c$, then they can be written as continuation of the expansion series at the nearest $\theta^*$ to the boundaries where $\bar{\lambda}(\theta^*) = c$; the above discussion remains true. When $d\bar{\lambda}/d\theta = 0$ at $\theta$, without too much restriction to the basic flow, a series expansion of the solution around $\theta$ would yield

$$\psi_1(\theta, c) = [c - \bar{\lambda}(\theta)]^{(\rho_1')}\phi_1(\theta, c), \quad (21)$$

and the second solution has the form (Korn and Korn 1968, chapter 9)

$$\psi_2(\theta, c) = g\psi_1(\theta, c)\ln\left[\bar{\lambda}(\theta) - c\right] + \left[c - \bar{\lambda}(\theta)\right]^{\rho_1}\phi_2(\theta, c). \quad (22)$$

If these functions are analytically extended to the boundaries, one finds that $G_1(\theta, c)$ in (A1) can be arranged to only contain $\{[c - \bar{\lambda}(\theta)][\bar{\lambda}(\theta_1) - c]\}^{\rho_1}$ and $\ln[(c - \bar{\lambda}(\theta))/(c - \bar{\lambda}(\theta_1))]$. It becomes a single-valued function with cut line connecting $c = \bar{\lambda}(\theta)$ and $c = \bar{\lambda}(\theta_1)$. Similar discussions can be applied to $G_2(\theta, c)$ and $D(c)$.

As a result, the cut lines of $G(\theta, \theta', c)$ can be taken as within $[\bar{\lambda}_{\min}, \bar{\lambda}_{\max}]$. For $\psi^k(\theta, c)$, these lines occupy the whole interval of $[\bar{\lambda}_{\min}, \bar{\lambda}_{\max}]$. The inverse Laplace integration around the interval (see Fig. 1b) is

$$\psi_c^k = \frac{1}{2\pi i}\oint_{C_r}\left[\int_0^\pi \frac{G^k(\theta, \theta', c)}{\bar{\lambda}(\theta') - c}\zeta_0^k(\theta')\, d\theta'\right]e^{-ikct}\, dc = \oint_{C_r}\left\{\left[\int_0^\theta E_1(\theta', c)\zeta_0^k(\theta')\, d\theta'\right]G_2^k(\theta, c) + \left[\int_0^\pi E_2(\theta', c)\zeta_0^k(\theta')\, d\theta'\right]G_1^k(\theta, c)\right\}e^{-ikct}\, dc, \quad (23)$$

where $E_1(\theta, c)$ and $E_2(\theta, c)$ can be derived as

$$E_1(\theta, c) = \frac{G_1(\theta, c)}{2\pi i D(c)W(\psi_1, \psi_2)\left(\bar{\lambda}(\theta) - c\right)}, \quad (24)$$

$$E_2(\theta, c) = \frac{G_2(\theta, c)}{2\pi i D(c)W(\psi_1, \psi_2)\left(\bar{\lambda}(\theta) - c\right)}. \quad (25)$$

Define

$$B^k(c)G^k(\theta, c) = \left[\int_{\theta_1}^\theta E_1(\theta', c)\zeta_0^k(\theta')\, d\theta'\right]G_2^k(\theta, c) + \left[\int_\theta^{\theta_2} E_2(\theta', c)\zeta_0^k(\theta')\, d\theta'\right]G_1^k(\theta, c). \quad (26)$$

It can be proven that $G^k(\theta, c)$ satisfies (18)–(19) when $c$ is on the contour $C_r$. Let contour $C_r$ approach line $[\bar{\lambda}_{\min}, \bar{\lambda}_{\max}]$, and (23) can be written as

$$\psi_c^k = \int_{\bar{\lambda}_{\min}}^{\bar{\lambda}_{\max}} B^k(c)G^k(\theta, c)e^{-ikct}\, dc. \quad (27)$$

Since $c$ varies continuously in the interval of $[\bar{\lambda}_{\min}, \bar{\lambda}_{\max}]$, $c \in [\bar{\lambda}_{\min}, \bar{\lambda}_{\max}]$ is defined as the continuous spectrum of the model. The associated $G^k(\theta, c)$ is the spectral functions of the continuum. Here $\psi_c^k$ is defined as the continuous spectrum disturbance. If the integration of (27) exists at $t = 0$, then $\psi_c^k$ approaches zero as time approaches infinity.

In summary, the solution of the initial value problem of (1), can be written as

$$\psi'(\lambda, \theta, t) = \psi'_d(\lambda, \theta, t) + \psi'_d(\lambda, \theta, t) = \sum_k \sum_l A_l^k G_l^k(\theta) e^{ik(\lambda - ct)} + \sum_k \int_{\bar{\lambda}_{\min}}^{\bar{\lambda}_{\max}} B^k(c) G^k(\theta, c) e^{ik(\lambda - ct)}\, dc. \quad (28)$$

The first part represents the discrete spectrum disturbance (modal solution) and the second part represents the continuous spectrum disturbance (nonmodal solution).

## 3. Distribution and bounds of discrete spectra and projection of arbitrary disturbances

We now consider the distribution of the discrete spectra of (18)–(19). The sufficient condition of barotropic stability states that, if $d\bar{\zeta}/d\theta$ has the same sign within the interval $[\theta_1, \theta_2]$, the only possible locations of all discrete spectral points are on the real axis (Kuo 1949). The general properties of the distribution of discrete spectra, for both the neutral and unstable ones, can be obtained only with very specific basic flow conditions (Dickinson and Clare 1973). For instance, when the basic flow is uniformly distributed, the classic phase speed formula of Rossby waves gives all the spectral values, and the Rossby–Haurwitz waves are the corresponding spectral functions. For general basic flow, Howard (1961) gave a semicircle theorem about the existing domain of discrete spectra. Pedlosky (1964b) gave several other bounds of the real and imaginary phase speeds. All of them were derived using constraints of integral quadratic properties. Taking a different approach, here we give another estimation of the existing domain that relates the discrete spectra to the basic flow and the gradient of its absolute vorticity.

For a particular spectral function $G_l^k(\theta)$ of the discrete spectra, let

$$Q_l^k(\theta) = \sin\theta \frac{d}{d\theta} \sin\theta \frac{dG_l^k}{d\theta} - k^2 G_l^k. \quad (29)$$

With the homogenous boundary condition, the inverse becomes

$$G_l^k(\theta) = \int_{\theta_1}^{\theta_2} G(\theta, \theta') Q_l^k(\theta') \sin^{-1}\theta'\, d\theta', \quad (30)$$

where Green's function

$$G(\theta, \theta') = \begin{cases} -\dfrac{1}{2k} \tan^k\left(\dfrac{\theta}{2}\right) \cot^k\left(\dfrac{\theta'}{2}\right) & \text{for } \theta \le \theta' \\ -\dfrac{1}{2k} \tan^k\left(\dfrac{\theta'}{2}\right) \cot^k\left(\dfrac{\theta}{2}\right) & \text{for } \theta > \theta'. \end{cases} \quad (31)$$

Thus, eigenvalue problem (18)–(19) can be rewritten into the following form,

$$\left(\bar{\lambda} - c\right) Q_l^k(\theta) - \sin\theta \frac{d\bar{\zeta}}{d\theta} \int_{\theta_1}^{\theta_2} G(\theta, \theta') Q_l^k(\theta') \sin^{-1}\theta'\, d\theta' = 0. \quad (32)$$

Because for every spectral point $|Q_l^k(\theta)|$ must assume a maximum at certain latitude $\theta_M$ in the interval $[\theta_1, \theta_2]$, we have

$$|\bar{\lambda}(\theta_M) - c| \le \left|\sin\theta \frac{d\bar{\zeta}}{d\theta}\right|_{\theta_M} \int_{\theta_1}^{\theta_2} |G(\theta_M, \theta')| \frac{|Q_l^k(\theta')|}{|Q_l^k(\theta_M)|} \sin^{-1}\theta'\, d\theta' \le \frac{\beta_M}{k^2}, \quad (33)$$

where

$$\beta_M = \max \left|\sin\theta \frac{d\bar{\zeta}}{d\theta}\right|.$$

The above inequality gives a bound to the imaginary part of the phase speed:

$$|c_i| \le \frac{\beta_M}{k^2}. \quad (34)$$

Bounds for the total phase speed can be given as

$$\bar{\lambda}_{\min} - \frac{\beta_M}{k^2} \le |c| \le \bar{\lambda}_{\max} + \frac{\beta_M}{k^2}. \quad (35)$$

Bounds from (33) are schematically shaded in Fig. 1c. They complement those in Howard (1961), Pedlosky (1964b), Watson (1981), and Thuburn and Haynes (1996). The upper bound of $c_r < \bar{\lambda}_{\max}$ in Pedlosky (1964b) is stronger than what can be derived from (35). However, in cases such as $d\bar{\zeta}/d\theta = 0$, $\beta_M = 0$, (34) is apparently stronger than those given in Pedlosky (1964b) and in Thuburn and Haynes (1996). It is noted here that virtually all previous bound estimations used the integral approach, with bounds expressed as functions of the maximum and mimimum of the basic zonal velocity or angular velocity. We have introduced a new approach that expresses the bounds as a function of the basic vorticity gradient.

With regard to the number of discrete spectrum points, we have a theorem: *There can be only limited number of spectral points for (18)–(19) beyond any arbitrary small neighbor of* $[\bar{\lambda}_{min}, \bar{\lambda}_{max}]$. This can be proved as follows. Let $c$ be a discrete spectral point; $c$ is then a zero point of $D$ in (A4). Since $D(c)$ is an analytic function of $c$, its roots are isolated and they do not form accumulation points. From the bounds, the spectral points can only exist in a limited domain. Since if a point series in a limited domain has no accumulation point the number of points must be limited, accumulation points of the spectra can only be in $c \in [\bar{\lambda}_{\min}, \bar{\lambda}_{\max}]$ if they exist. Note that this is consistent with results

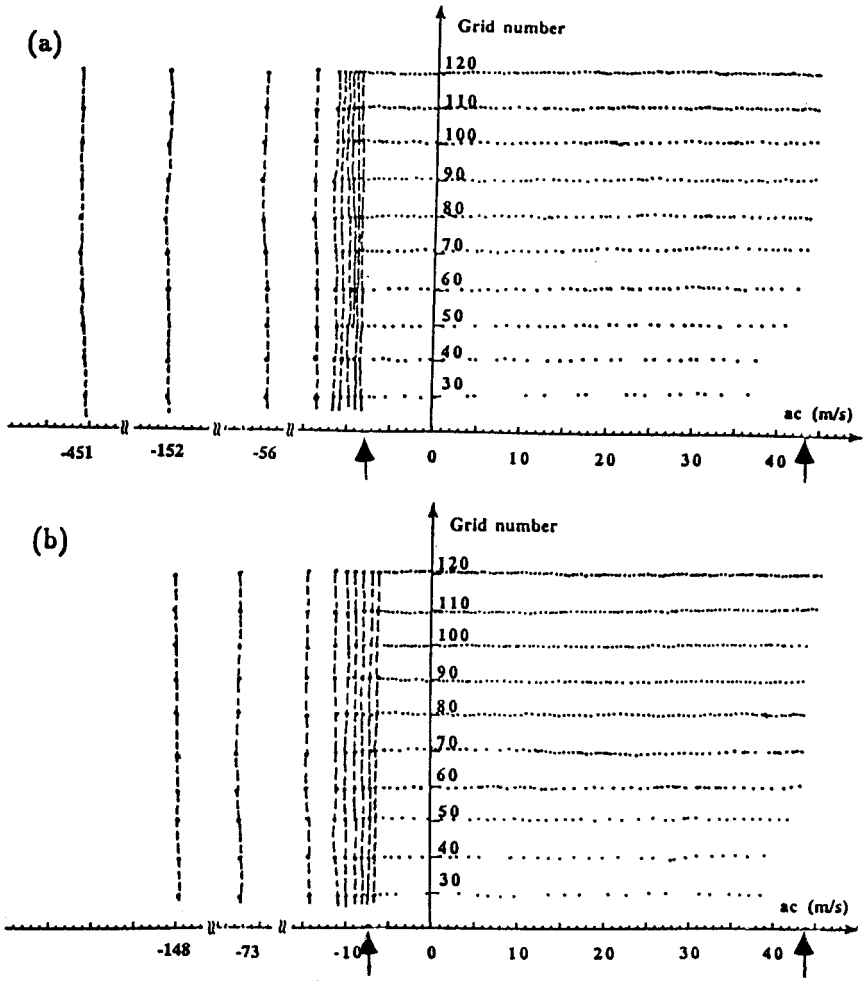


FIG. 2. Distribution of calculated spectra for different resolutions using observed zonal mean flow at 300 mb in October 1982. The ordinate gives the number of grids. The abscissa is the spectral values multiplied by the radius of the earth *a*. Arrows indicate maximum and minimum angular velocity of the basic flow multiplied by *a*. (a) For zonal wavenumber $k = 1$. (b) For zonal wavenumber $k = 2$.

reported in Kasahara (1980), Dikiy and Katayev (1971), and Farrell (1989). It should be also noted that within an infinitesimal neighbor of $[\bar{\lambda}_{\min}, \bar{\lambda}_{\max}]$, there could be infinite number of spectral points. An example is the infinite number of Rossby waves under constant $\bar{\lambda}$ where the infinite number of these waves have phase speeds in the small neighbor of $\bar{\lambda}$.

It can also been shown that, spectral functions of the discrete spectra of (18)–(19) are weighted orthogonal to each other (Held 1985; Lu et al. 1986). Let $c_l^k$ and $c_{l'}^k$ be two different spectra; their associated spectral functions satisfy

$$(c_l^k - c_{l'}^k) \int_{\theta_1}^{\theta_2} \frac{Q_l^k(\theta) Q_{l'}^k(\theta)}{d\bar{\zeta}/d\theta} \sin\theta \, d\theta = 0, \qquad (36)$$

where $Q_l^k$ is defined as in (29). Then $G_l^k(\theta)$ can be normalized such that

$$\int_{\theta_1}^{\theta_2} \frac{Q_l^k(\theta) Q_l^k(\theta)}{d\bar{\zeta}/d\theta} \sin\theta \, d\theta = 1. \qquad (37)$$

Then an initial disturbance can be projected onto $G_l^k$ with the projection coefficient as

$$A(c_l^k) = \int_{\theta_1}^{\theta_2} \frac{\zeta_0'(\theta) Q_l^k(\theta)}{d\bar{\zeta}/d\theta} \sin\theta \, d\theta. \qquad (38)$$

TABLE 1. Number of neutral discrete spectral points in the four seasons of 1982.

| Wavenumber | 1 | 2 | 3 | 4 | 5 | 6 | 7 | 8 | 9 | 10 |
|---|---|---|---|---|---|---|---|---|---|---|
| January | 8 | 8 | 7 | 6 | 6 | 5 | 5 | 4 | 4 | 4 |
| April | 10 | 8 | 7 | 7 | 6 | 6 | 5 | 5 | 5 | 4 |
| July | 8 | 7 | 6 | 6 | 5 | 4 | 4 | 4 | 4 | 3 |
| October | 10 | 9 | 8 | 8 | 6 | 6 | 6 | 6 | 6 | 6 |

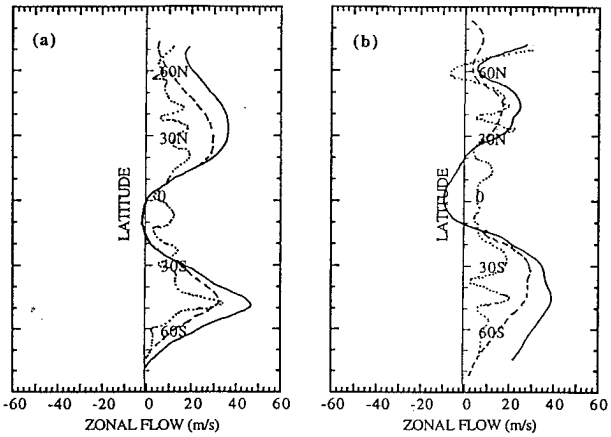


FIG. 3. Latitudinal distribution of the zonal mean basic westerly $\bar{v}_\lambda$ (m/s) (dashed) at 300 mb in 1982, the associated angular velocity multiplied by $a$ in m s$^{-1}$ (solid), and the nondimensionalized $-d\bar{\zeta}/d\theta$ (dotted) for (a) January and (b) July.

## 4. Calculation of spectra and spectral functions (finite difference approximation)

Let $y = \cos\theta$; (18) takes the form of

$$\left(\bar{\lambda} - c\right)\left[\frac{d}{dy}(1 - y^2)\frac{d}{dy} - \frac{k^2}{1 - y^2}\right]G + G\frac{d}{dy}\left[2\omega a y - \frac{d}{dy}(1 - y^2)\bar{\lambda}\right] = 0, \quad (39)$$

where, $y \in [-1, +1]$. We then divide $y \in [-1, 1]$ by $J$ grid points $y_j$ ($j = 2, 3, \ldots, J + 1$) with a constant resolution $\Delta y = 2/(J + 1)$ and $y_1 = -1$, $y_{J+2} = 1$. Denoting $G_j = G(y_j)$ and using the boundary conditions, we have

$$(\bar{\lambda}\mathbf{I} - c\mathbf{I})\,\mathbf{AG} + \mathbf{PG} = 0. \quad (40)$$

Here $\mathbf{I}$ is the unit matrix, and

$$\mathbf{G} = (G_2, G_3, G_4, \ldots, G_{J+1})^T. \quad (41)$$

Also, $\bar{\lambda}$, $\mathbf{A}$ and $\mathbf{P}$ are all matrices. For a given basic flow, (40) can be solved to obtain spectra $cs$ and spectral vectors $G_s$ of the model.

The range of continuous spectrum of $[\bar{\lambda}_{\min}, \bar{\lambda}_{\max}]$, as discussed in section 2, can then be used to categorize the calculated spectra into numerically distorted continuous spectrum and true discrete spectra. This distinction is also supported by previous numerical studies, with an increasing number of grid points, beyond certain extent of resolution, the numerically added spectral points all locate within the interval of $[\bar{\lambda}_{\min}, \bar{\lambda}_{\max}]$ (e.g., Lu et al. 1986).

The validity of this phenomenon under spherical geometry and realistic general basic flow is shown in Fig. 2. We gradually increase the grids from the North Pole to the South Pole by increments of 10 per calculation, starting at 30 and going to 120. Figures 2a and 2b show the distribution of calculated spectra for zonal wavenumber $k = 1$ and $k = 2$. The ordinate is the number of grid points. The basic flow taken here is the 300-mb mean zonal wind in October 1982. The basic flow satisfies the barotropic stable criteria, so we did not obtain complex spectra in this figure. It is seen that, with the increase of resolution, the number of calculated spectral points outside the interval of $[\bar{\lambda}_{\min}, \bar{\lambda}_{\max}]$ is indeed fixed. There are ten and nine neutral modes for zonal wavenumber $k = 1$ and $k = 2$, respectively. Their values change little with different $\Delta y$, and they approach their own limits as the resolution in increased. The added points in the course of increasing resolution are all lo-

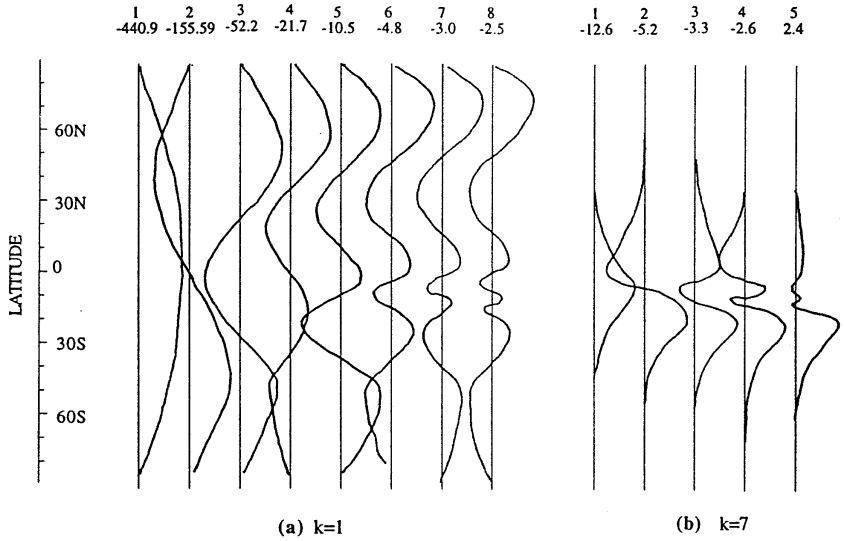


FIG. 4. Spectral functions of discrete spectra using January basic flow in Fig. 3a for zonal wavenumbers $k = 1$ (a) and $k = 7$ (b). Value listed above each function is the corresponding spectral value multiplied by the radius of the earth (unit in m s$^{-1}$).

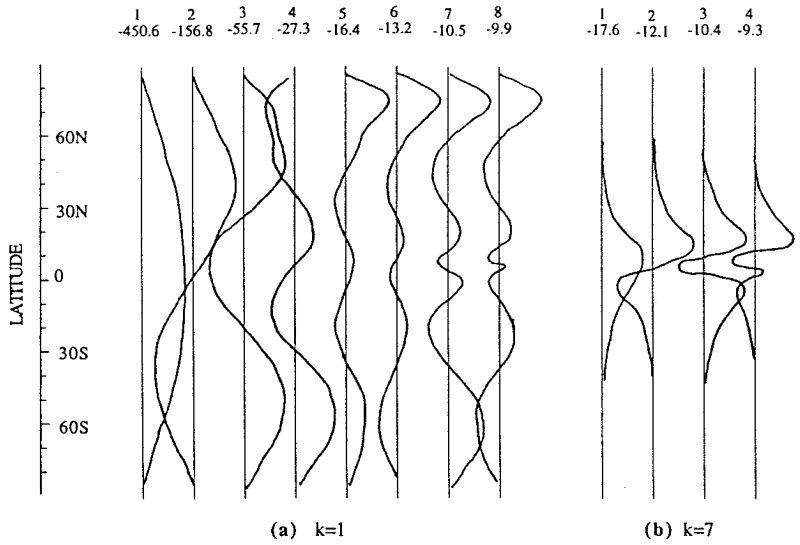


FIG. 5. Spectral functions of the neutral discrete spectra using the July basic flow in Fig. 3b for zonal wavenumbers $k = 1$ (a) and $k = 7$ (b). Value listed above each function is the corresponding spectral value multiplied by the radius of the earth (unit in m $s^{-1}$).

cated within the interval of of $[\bar{\lambda}_{\min}, \bar{\lambda}_{\max}]$. The features illustrated here are common for basic flows in other seasons (figures not shown). In particular, for an unstable basic flow, the number of unstable spectral points is also fixed, and they also approach their limits as the resolution is increased. In association with the convergence of computed discrete spectra, the corresponding spectral functions approach their limit functions too.

Since the result of this procedure is consistent with the analysis in section 2, we can safely consider the numerical spectral points outside $[\bar{\lambda}_{\min}, \bar{\lambda}_{\max}]$ as the discrete spectra of the differential equation and those points within $[\bar{\lambda}_{\min}, \bar{\lambda}_{\max}]$ as a sample set in the continuous spectrum. We have computed the spectra and spectral functions for different basic flows taken from the 300-mb mean zonal flow in the four seasons of 1982. The results are similar for different seasons as far as the major properties of discrete and continuous spectra are concerned. As a consequence, most of our discussions in the following sections focus on the winter and summer seasons.

## 5. Discrete spectra and structure of spectral functions

Table 1 lists the number of neutral discrete spectral points for different zonal wavenumbers in the four seasons. It is seen that, in all cases the number is no more than 10. The number decreases with the increase of zonal wavenumber. Figure 3a gives the profile of mean basic westerly $\bar{v}_\lambda$ (m $s^{-1}$) in January 1982 and the associated scaled angular velocity $\bar{\lambda}$ ($= a\bar{\lambda}$ in m $s^{-1}$). Also plotted is the gradient of the absolute vorticity of the basic flow. Figures 4a and 4b show the corresponding discrete spectral functions for zonal wavenumber $k = 1$ and $k = 7$, respectively. The values of spectral points are given above each spectral function (in terms of $c$ multiplied by the radius of the earth $a$). These functions represent the normal modes (characteristic waves). Each of them is a free wave that is able to propagate at a constant phase speed in the basic flow without changing its shape.

It is seen that, for zonal wavenumber $k = 1$, spectral functions of all calculated discrete spectra have global structures, with the maxima being at midlatitude. This implies that a freely traveling ultralong wave, in accordance with its zonal wavelength, also extends to all latitudes in the meridional direction. Along with the increase of spectral value, that is, increase of phase speed, the number of zero points of the spectral functions increases. For zonal wavenumber $k = 7$, the discrete spectral functions show quite different structures in comparison with those for wavenumber $k = 1$. All of the five spectral functions are visibly large only in

TABLE 2. Unstable modes in July 1982 (unit in m $s^{-1}$).

| k | 1 | 2 | 3 | 4 | 5 | 6 | 7 | 8 | 9 | 10 |
|---|---|---|---|---|---|---|---|---|---|---|
| $ac_r$ | 7.56 | None | 6.16 | 6.88 | 7.04 | None | None | None | None | None |
| $ac_i$ | ±0.74 | | ±1.34 | ±1.11 | ±0.63 | | | | | |
| $ac_r$ | 11.26 | None | None | 9.86 | 10.37 | None | None | None | None | None |
| $ac_i$ | ±0.52 | | | ±0.35 | ±0.72 | | | | | |

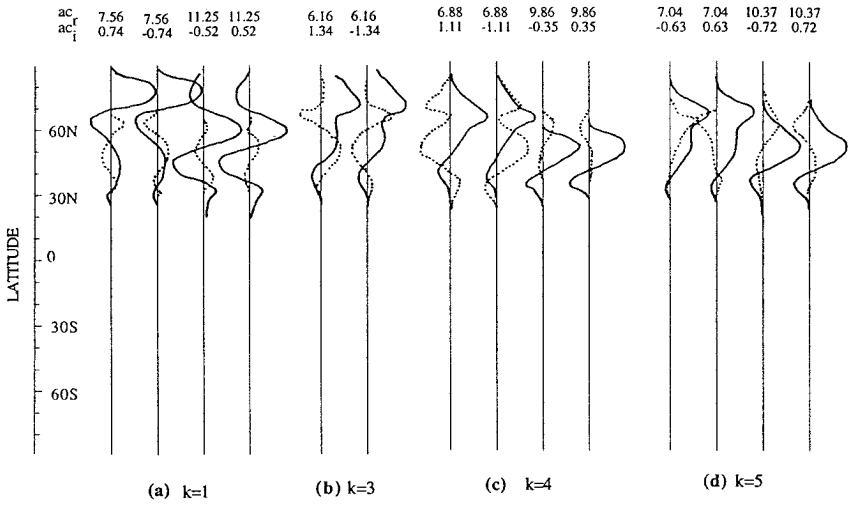


FIG. 6. Spectral functions of unstable discrete spectra using July basic flow in Fig. 3b for different zonal wavenumbers. Solid and dotted lines are real and imaginary parts of the spectral functions. Value listed above each function is the corresponding spectral value multiplied by the radius of the earth (unit in m $s^{-1}$).

low latitudes, implying that the synoptic-scale (large $k$) traveling waves can only exist in the Tropics.

The mean 300-mb basic flow for July 1982 is given in Fig. 3b. It is seen that in the Northern Hemisphere there is an interval where the gradient of absolute basic vorticity $-d\bar{\zeta}/d\theta \leq 0$, although the domain is small. At other latitudes, $-d\bar{\zeta}/d\theta > 0$. It follows from the barotropic instability criterion that the basic flow may be unstable. Indeed, we obtained unstable modes in the calculation.

Figures 5a and 5b show the structure of spectral functions of neutral discrete spectra for zonal wavenumber $k = 1$ and $k = 7$ in the July case. The qualitative characteristics are the same as in the winter case. There are eight neutral modes with global extension for $k = 1$, and four modes prevailing in the Tropics for $k = 7$.

As another subset of the discrete spectra, Table 2 lists the number and value of unstable spectral points for different zonal wavenumbers. It is seen that, for any zonal wavenumber, the maximum possible number of unstable modes does not exceed two conjugate pairs. The fastest increasing rate occurs at $k = 3$ and 4, corresponding to an $e$-folding time of 18.34 and 16.45 days, respectively. Thus, the developing and decaying of unstable modes are actually very slow, and they cannot account for the typically observed development and decay of atmospheric disturbances.

Figure 6 shows the spectral functions for the unstable modes in Table 2. The heavy line is the real part of the complex function and the dotted line is the imaginary part. One thing to note is that they differ greatly from the neutral discrete spectral modes. They only have very localized structures, just around the area where $-d\bar{\zeta}/d\theta < 0$. The unstable modes are fully absent in the Southern Hemisphere where $-d\bar{\zeta}/d\theta > 0$.

## 6. Spectral functions associated with the continuous spectrum

The computed spectra of distorted continuous spectrum are located within the interval of $[\bar{\lambda}_{\min}, \bar{\lambda}_{\max}]$. Figures 7a and 7b show the calculated spectral functions for zonal wavenumbers $k = 1$ and $k = 7$ using the January basic flow given in Fig. 3a. The corresponding spectral values are also listed above the spectral functions. The locations of jets in the two hemispheres, where $\bar{\lambda}$ reaches maximum, are indicated with J. It is clear that, for a specific spectral value $c$, the spectral function has a sharp turning at critical latitude $\theta_c$, where zonal angular velocity $\bar{\lambda}(\theta_c)$ is equal to $c$. The structures of these functions are localized and are mainly restricted within a limited latitudinal zone where $\bar{\lambda}(\theta) > c$. In the area where $\bar{\lambda}(\theta) < c$, they either equal to zero or exponentially and rapidly decrease from the critical latitude. As a result, the larger the spectral value $c$, the narrower the visible domain of the spectral function. Since the two prevailing westerlies, one in each hemisphere, are separated by the tropical easterlies, spectral functions of the continuous spectrum are composed of two branches, one in each of the hemispheres. Furthermore, with the increase of zonal wavenumber $k$, even in one westerly branch, or one hemisphere, spectral functions of the continuous spectrum split into two groups, separately located on the two sides of the jet core but confined within the two critical latitudes (see Fig. 7b).

Figures 8a and 8b are the computed spectral functions of continuous spectrum corresponding to the July basic flow of Fig. 3b. Qualitatively, they are similar to those given in Fig. 7. All the functions exhibit very localized structures.

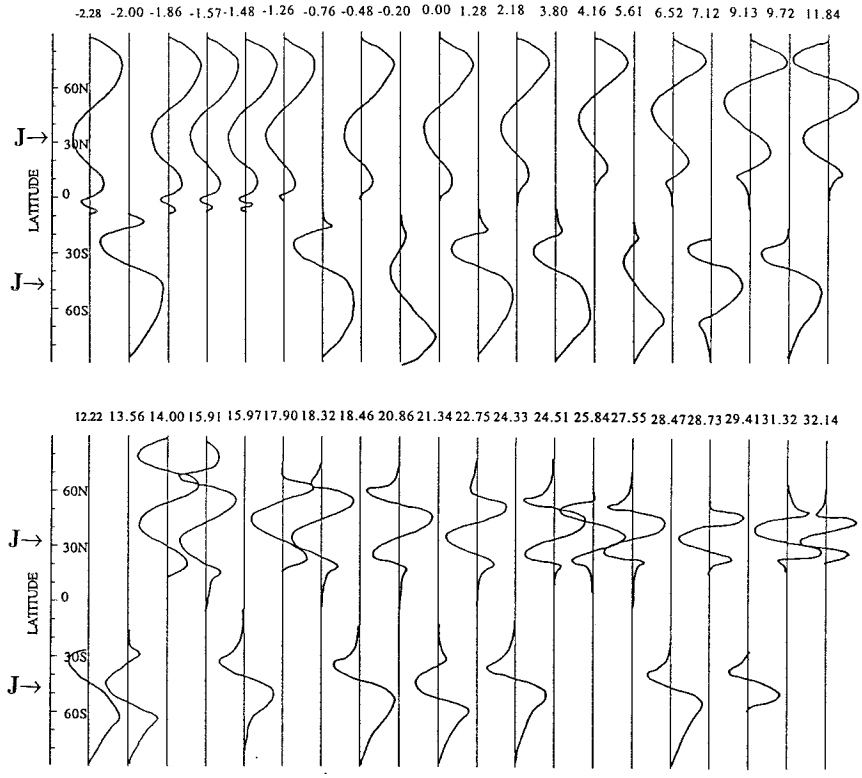


FIG. 7a. Same as Fig. 4a (wavenumber 1, January 1982), except for a sample of continuous spectrum. Note "J" marks locations of the jets.

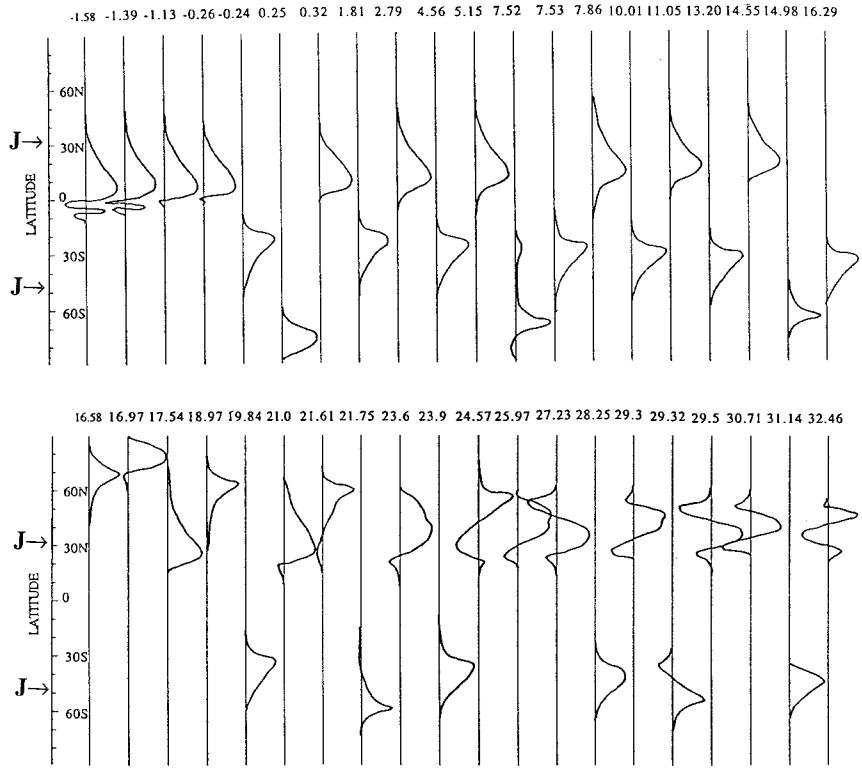


FIG. 7b. Same as Fig. 7a except zonal wavenumber 7.

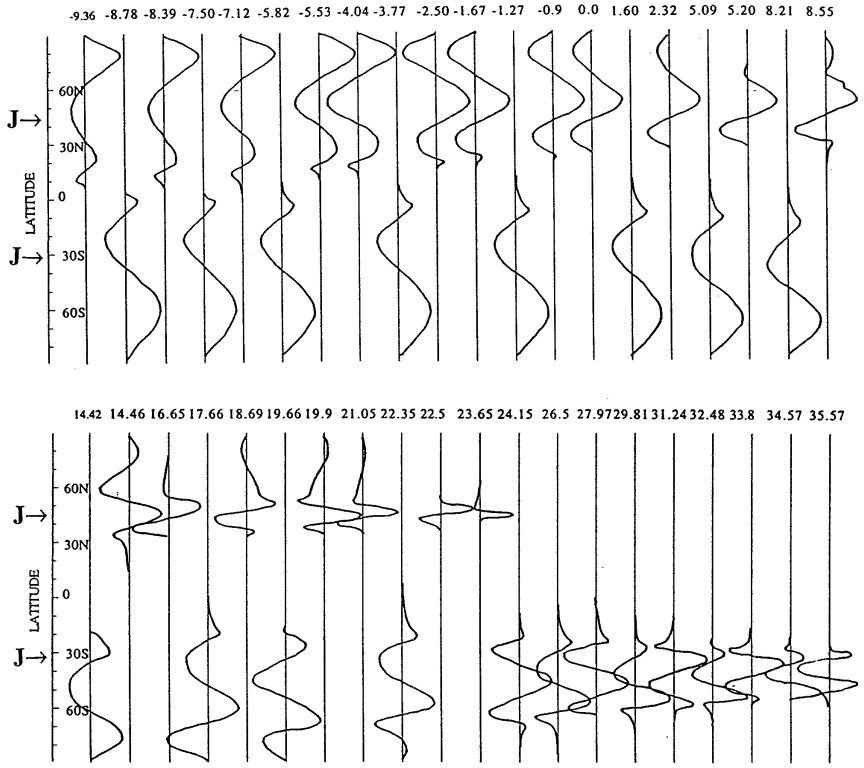


FIG. 8a. Same as Fig. 5a (wavenumber 1, July 1982), except for a sample of continuous spectrum. Letter ''J'' marks locations of the jets.

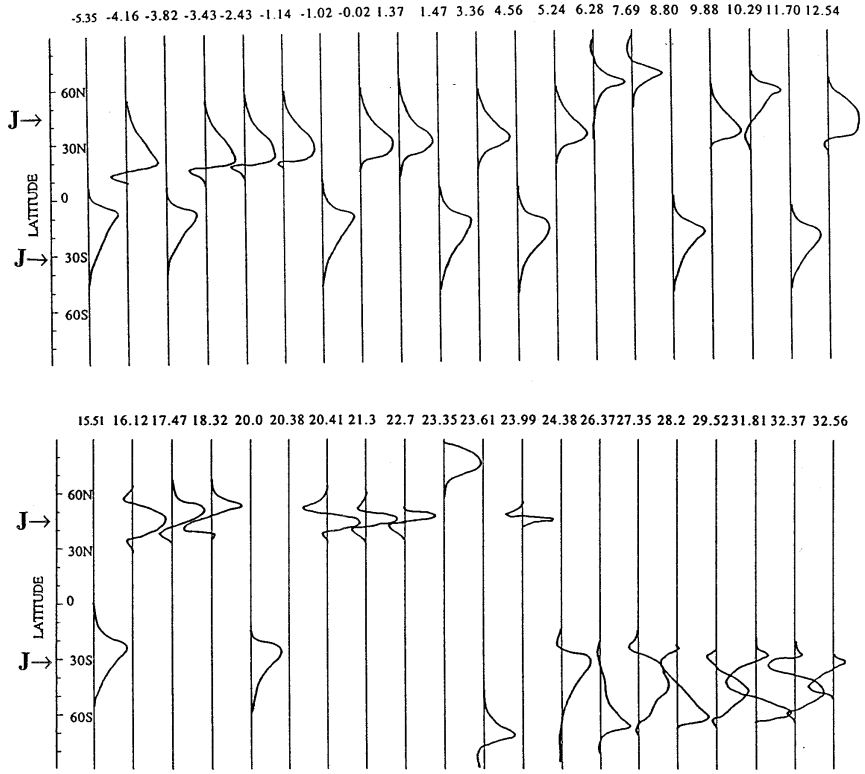


FIG. 8b. Same as Fig. 8a except wavenumber 7.

The structures of spectral functions of the continuous spectrum suggest neither direct interaction of the majority of eddies between the two hemispheres, nor direct interaction of the synoptic-scale disturbances at the two sides of the jet stream.

## 7. Summary and conclusions

Using the barotropic quasigeostrophic vorticity model, we have presented a formulation of the evolution of small disturbances superimposed on an arbitrary basic flow. Part of the evolution is represented by the discrete spectra of the model that is consistent with traditional normal modes in time and space. The other part is represented by model continuum that covers the range of minimum to maximum zonal angular velocities. While each mode in the first part is capable of propagating freely in the atmospheric zonal basic flow, disturbances represented by the second part approach zero as time tends to infinity. The theoretical analysis is then used to interpret the numerical calculation of discrete and continuous spectra of the model using realistic atmospheric basic zonal flow at 300 mb in the four seasons of 1982.

For a given zonal wavenumber, the number of discrete spectra that represent free or exponentially developing or decaying waves in the basic flow is limited. The number of neutral discrete spectral points changes from about 10 for ultralong waves, which also extend globally in the meridional direction, to 5 for synoptic waves, which are restricted in the Tropics. The structures of unstable modes, although they belong to the discrete spectra, are shown to differ dramatically from the neutral discrete modes. They have very localized structures but with developing or decaying timescales longer than 2 weeks.

All of the calculated continuous spectral functions exhibit first-order discontinuities at latitudes where their spectral value (phase speed) is equal to that of the basic flow, that is, at the so-called critical latitude. They are localized in midlatitudes with their amplitudes extending from the critical latitudes toward the side where basic flow is larger than their spectral values. Two branches of continuous spectral functions are found to locate separately in the two westerlies of the Northern and Southern Hemispheres. With the increase of zonal wavenumber, spectral functions within one westerly (i.e., in one hemisphere) further split into two subbranches locating separately on the two sides of the jet core (maximum angular velocity of the zonal flow) but within the two corresponding critical latitudes. These structures, when used as integrand to form the continuum solution, provide the basis to study the nonmodal motions of atmospheric disturbances.

*Acknowledgments.* This research was partly supported by NASA Grant NAGW3517 and DOE Grant DEFG0285-ER60314 to SUNY at Stony Brook. Additional support was provided by the Chinese Program on Basic Research and by the Institute of Atmospheric Physics, Academia Sinica. We thank the two anonymous reviewers whose critical comments have led to many improvements to the original manuscript. We are also very grateful to the editor, Dr. Joe Tribbia, who reviewed the manuscript in great detail and uncovered a mathematical error in the original manuscript.

## APPENDIX

## The Green's Function

Given $\psi_1(\theta, c)$ and $\psi_2(\theta, c)$ as two independent solutions of the homogeneous form of Eq. (7), which are all analytic functions of $c$, the Green's function of (7) can be written as

$$G^k(\theta, \theta', c) = \begin{cases} \dfrac{G_1(\theta', c)G_2(\theta, c)}{D(c)W(\psi_1, \psi_2)}, & \text{if } \theta \geq \theta' \\ \dfrac{G_1(\theta, c)G_2(\theta', c)}{D(c)W(\psi_1, \psi_2)}, & \text{if } \theta < \theta', \end{cases} \tag{A1}$$

where

$$G_1(\theta, c) = \psi_2(\theta_1, c)\psi_1(\theta, c) - \psi_1(\theta_1, c)\psi_2(\theta, c), \tag{A2}$$

$$G_2(\theta, c) = \psi_2(\theta_2, c)\psi_1(\theta, c) - \psi_1(\theta_2, c)\psi_2(\theta, c), \tag{A3}$$

$$D(c) = \psi_1(\theta_1, c)\psi_2(\theta_2, c) - \psi_1(\theta_2, c)\psi_2(\theta_1, c). \tag{A4}$$

Here $W(\psi_1, \psi_2)$ is the Wronski determinant given as

$$W(\psi_1, \psi_2) = \psi_1\frac{d\psi_2}{d\theta} - \psi_2\frac{d\psi_1}{d\theta}. \tag{A5}$$

Here $W \neq 0$ and it is independent of $\theta$ and $c$. Apparently, $G_1(\theta, c)$ and $G_2(\theta, c)$ satisfy the homogeneous form of Eq. (7). Furthermore, they satisfy the following boundary conditions,

$$G_1(\theta, c)\big|_{\theta=\theta_1} = 0 \tag{A6}$$

$$G_2(\theta, c)\big|_{\theta=\theta_2} = 0. \tag{A7}$$

Because $D(c)$ can only have isolated roots beyond $c \in [\bar{\lambda}_{\min}, \bar{\lambda}_{\max}]$, the Green's function $G^k(\theta, \theta', c)$ only has removable singularities beyond $[\bar{\lambda}_{\min}, \bar{\lambda}_{\max}]$.

## REFERENCES

Burger, A. P., 1966: Instability associated with continuous spectrum in a baroclinic flow. *J. Atmos. Sci.*, **23,** 272–277.

Case, K. M., 1960: Stability of inviscid plane couette-flow. *Phys. Fluids,* **3,** 143–1148.

Charney, J. G., 1947: The dynamics of long waves in a baroclinic westerly current. *J. Meteor.*, **4,** 125–162.

Dickinson, R. E., and F. J. Clare, 1973: Numerical study of the unstable modes of a hyperbolic-tangent barotropic shear flow. *J. Atmos. Sci.*, **30,** 1035–1049.

Dikiy, L. A., and V. V. Katayev, 1971: Calculation of the planetary wave spectrum by the Galerkin method. *Atmos. Oceanic Phys.*, **7,** 1031–1038.

Farrell, B. F., 1982: The initial growth of disturbances in a baroclinic flow. *J. Atmos. Sci.,* **39,** 1663–1686.

——, 1985: Transient growth and damped baroclinic waves. *J. Atmos. Sci.,* **42,** 2718–2727.

——, 1989: Optimal excitation of baroclinic waves. *J. Atmos. Sci.,* **46,** 1193–1206.

Held, I. M., 1985: Pseudomomentum and the orthogonality of modes in shear flows. *J. Atmos. Sci.,* **42,** 2280–2288.

——, R. L. Panetta, and R. T. Pierrehumbert, 1985: Stationary external Rossby waves in vertical shear. *J. Atmos. Sci.,* **42,** 865–883.

Howard, L. N., 1961: Note on a paper by John W. Miles. *J. Fluid Mech.,* **10,** 509–512.

Kasahara, A., 1980: Effect of zonal flow on the free oscillations of a barotropic atmosphere. *J. Atmos. Sci.,* **37,** 917–929.

Korn, G. A., and T. M. Korn, 1968: *Mathematical Handbook for Scientists and Engineers.* McGraw-Hill, 1129 pp.

Kuo, H. L., 1949: Dynamic instability of two-dimensional non-divergent flow in a barotropic atmosphere. *J. Meteor.,* **6,** 105–122.

Lu, P. S., L. Lu, and Q. C. Zeng, 1986: Spectra of the barotropic quasi-geostrophic model and the evolutionary process of disturbances. *Sci. Sin.* **11,** 1225–1233.

Pedlosky, J., 1964a: An initial value problem in the theory of baroclinic instability. *Tellus,* **16,** 12–17.

——, 1964b: The stability of currents in the atmosphere and the ocean: Part I. *J. Atmos. Sci.,* **21,** 201–219.

Thuburn, J., and P. H. Haynes, 1996: Bounds on the growth rate and phase velocity of instabilities in non-divergent barotropic flow on a sphere: A semicircle theorem. *Quart. J. Roy. Meteor. Soc.,* **122,** 779–787.

Tung, K. K., 1983: Initial-value problems for Rossby waves in a shear flow with critical level. *J. Fluid Mech.,* **133,** 443–469.

Watson, M., 1981: Shear instability of differential rotation in stars. *Geophys. Astrophys. Fluid Dyn.,* **16,** 285–298.

Yamagata, T., 1976: On trajectories of Rossby wave packets released in a lateral shear flow. *J. Oceanol. Soc. Japan,* **32,** 162–168.

Yanai, M., and T. Nitta, 1968: Finite difference approximation for the barotropic instability problem. *J. Meteor. Soc. Japan,* **46,** 389–403.

Zeng, Q. C., 1979: *The Mathematical-Physical Basis of Numerical Weather Prediction.* Vol. 1, Science Press, 543 pp.

——, P. S. Lu, R. F. Li, and C. G. Yuan, 1986: Evolution of large scale disturbances and their interactions with mean flow in a rotating atmosphere, Part 1. *Adv. Atmos. Sci.,* **3,** 38–58.